

ANALYTICAL, NUMERICAL AND EXPERIMENTAL VALIDATION OF COIL VOLTAGE IN INDUCTION MELTING PROCESS

B Patidar, M.T.Saify, M.M.Hussain, S.K.Jha, and A.P.Tiwari

Bhabha Atomic Research Centre, Mumbai

ABSTRACT

This paper presents, mathematical model of induction heating process by using analytical and numerical methods. In analytical method, series equivalent circuit (SEC) is used to represent induction coil and work piece. Induction coil and workpiece parameters (resistance and reactance) are calculated by standard formulas along with Nagaoka correction factors and Bessel functions. In Numerical method, magnetic vector potential formulation is done and finite element method (FEM) is used to solve the field equations. Analytically and numerically computed parameters such as equivalent coil resistance, reactance, coil voltage, work piece power are compared and found that they are in good agreement. Analytically and numerically obtained coil voltages at different frequencies are validated by experimental results. This mathematical model is useful for coil design and optimization of induction heating process.

KEYWORDS: -

Electromagnetic, FEM, induction coil parameter, induction heating

1. INTRODUCTION

Induction heating is widely utilized in different industrial applications such as melting, forging, welding, hardening etc [1, 2]. It is based on electromagnetic induction phenomenon, which is very complex and results completely depend upon various design and process parameters [3]. Often, many experiments need to be conducted to optimize the melting process, which is expensive and time consuming. Mathematical modeling and simulation of induction melting process not only helps to avoid tedious experiments, it also helps to understand the process in depth.

Most of literature on induction heating system design and optimization are based on mathematical modeling and simulation [4]-[8]. Only few articles [9][10][11] are available, in which analytical methods are used to explain the induction heating process. In this paper, Analytical and numerical methods are used to calculate the coil voltages at different frequencies and validated it with experimental results.

In Analytical method, Nagaoka short coil correction factor is used to account the end effect and flux density outside the coil. Nagaoka modified correction factor is included in formulation to account presence of work piece inside the coil [6]. Lead resistance and inductance are significant, therefore they are also included in computation. Work piece resistance and power are calculated by using Bessel function, because it gives more accurate values compared to generalized formulas

[6]. Coil equivalent inductance is used to select proper values of capacitors for coil tuning with power source [1]. Analytical methods are generally applicable to simple geometries.

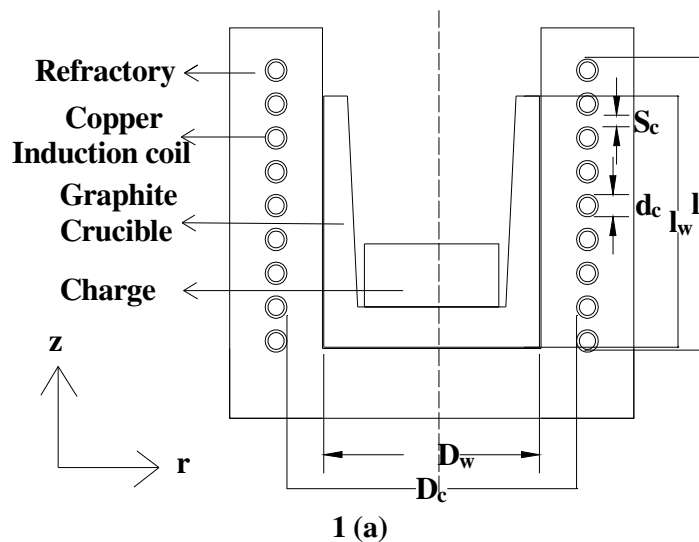
In Numerical method, magnetic vector potential formulation is used for computation of different design parameters. Magnetic vector potential formulation requires less computation compared to magnetic field formulation. Finite element method (FEM) based multiphysics software is used to solve the field equations and compute various parameters such as coil impedance, voltage and work piece power at different frequencies. Numerical methods can be applied to complicated geometry, but it requires detailed understanding of coding language. Numerical methods are iteration based and require lot of computation resources and time to solve the problem.

This paper is organized as follows: After introduction in section I, section II includes analytical formulation which is used to calculate various parameters such as coil equivalent resistance, reactance, coil voltage, work piece power, and coil efficiency. Mathematical model, numerical method, simulation procedure and experimental set up details are also explained in section II. In section III, all results computed from analytical and numerical method are displayed, analyzed and validated with experimental results.

2. METHODS

2.1 Analytical formulation

2-D Axisymmetric geometry of induction melting process is shown in figure 1 (a). Here, graphite crucible is placed inside the multi turn copper induction coil. Graphite is used as a susceptor and it heats up the charge by radiation and conduction. In induction melting process, Induction coil and workpiece can be represented by using series equivalent circuit (SEC) as shown in figure 1(b).



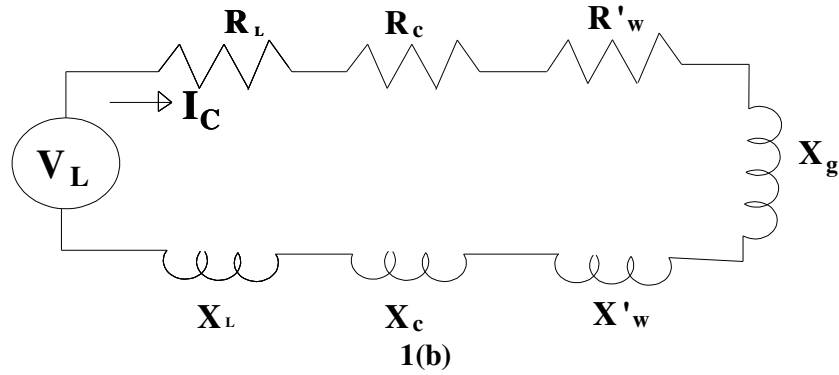


Figure 1(a) 2-D geometry of induction coil and workpiece. 1(b). Series equivalent circuit of Coil and workpiece (Graphite crucible)

In Series equivalent circuit, V_L is the coil voltage (V), I_c is the coil current (A), R_c is the coil resistance (Ω), X_c is the coil reactance (Ω), R_w is the work piece resistance (Ω), X_w is the work piece reactance (Ω), X_L is the lead reactance (Ω), R_L is the lead resistance (Ω), R'_w is the work piece resistance referred to coil side (Ω), X_g is air gap reactance (Ω), X'_w is work piece reactance referred to coil side (Ω).

Coil equivalent impedance (Z_{eq}) and coil voltage (V_L) are expressed by eq (1.1) and eq (1.2) respectively,

$$Z_{eq} = \sqrt{(R_{lead} + R_c + R'_w)^2 + (X_{lead} + X_c + X'_w + X_g)^2} \quad (1.1)$$

$$V_L = I_c Z_{eq} \quad (1.2)$$

Coil and workpiece parameters are calculated [9], [11] by using following formulas,

$$\text{Coil resistance } R_c = \frac{\pi(D_c + \delta_c)N_c^2 \rho_c}{\delta_c l_c k_r} \quad (2.1)$$

$$\text{Space factor } k_r = \frac{D_c N_c}{l_c} \quad (2.2)$$

$$\text{Coil skin depth } \delta_c = \sqrt{\frac{\rho_c}{\pi \mu_0 \mu_r f}} \quad (2.3)$$

In these equations, N_c is the no of turns, l_c is the coil height (m), D_c is the coil diameter (m), ρ_c is the copper resistivity ($\Omega\text{-m}$) at 393⁰K, μ_0 is the permeability of free space i.e. $4\pi \times 10^{-7}$, μ_r is the relative permeability ($\mu_r = 1$ for copper, graphite), f is the power source frequency (Hz).

$$\text{Coil reactance for } (t_c > 2\delta_c) \quad X_c = R_c \quad (3)$$

In this equation, t_c is coil tube thickness (m)

$$\text{Air gap reactance } X_g = \frac{k_n^* \mu_0 N_c^2 \pi^2 f (D_c^2 - D_w^2)}{2l_c} \quad (4.1)$$

$$k_n^* = k_n \left(1 - \left[\frac{D_w - \delta_w}{(D_c + \delta_c)} \right]^2 \right) + \left[\frac{D_w - \delta_w}{(D_c + \delta_c)} \right]^2 \quad (4.2)$$

$$k_n = \frac{1}{\left[1 + \frac{0.4502(D_c + \delta_c)}{l_c} \right]} \quad (4.3)$$

In these equations, D_w is the workpiece diameter (m), δ_w is the workpiece skin depth (m), k_n^* is the modified Nagaoka correction factor, k_n is the short coil correction factor.

Workpiece resistance and reactance are calculated by using workpiece active and reactive power respectively.

Workpiece active and reactive power is calculated by,

$$P_w = (\pi f \mu_0 \mu_r) l_w \left(\frac{\pi D_w^2}{2} \right) H^2 p \quad (5)$$

$$Q_w = (\pi f \mu_0 \mu_r) l_w \left(\frac{\pi D_w^2}{2} \right) H^2 q \quad (6)$$

Here, l_w = Workpiece length (m)

p, q = Workpiece power loss constant, this parameters are find out using equations given in [2],

H = Magnetic field intensity (A/m)

Magnetic field intensity is calculated by,

$$H = \frac{k_n^* NI}{l_c} \quad (7)$$

Lead resistance is calculated by standard ohms law considering the skin effect and proximity effect. Lead reactance is calculated by using parallel transmission line formula.

2.2 Mathematical modeling

Induction heating is multiphysics process i.e combination of Electromagnetic field and heat transfer. Electromagnetic field produced by induction coil is represented by maxwell equations [4]-[8], [15], [16],[17] as shown below,

$$\nabla \times \vec{H} = \sigma \vec{E} + \vec{j}^s \quad (8.1)$$

$$\nabla \times \vec{E} = - \frac{\partial \vec{B}}{\partial t} \quad (8.2)$$

$$\nabla \cdot \vec{B} = 0 \quad (8.3)$$

Constitutive equations,

$$\vec{B} = \mu_0 \mu_r \vec{H} \quad (8.4)$$

$$\vec{j} = \sigma \vec{E} \quad (8.5)$$

In these equations, H is the Magnetic field strength (A/m), E is the Electric field strength (V/m), σ is the Electrical conductivity (S/m), j^s is the source current density (A/m²), B is the Magnetic flux density (T). From eq (8.3), magnetic vector potential is defined as,

$$\vec{B} = \nabla \times \vec{A} \quad (9)$$

eq (8.4), eq (9) put into eq (8.1) gives,

$$\nabla \times \nabla \times \vec{A} = \mu_0 \mu_r (\sigma \vec{E} + \vec{j}^s) \quad (10)$$

From eq (8.2), eq (9) and by applying vector identity, eq (10) can be written as,

$$\nabla^2 A = \mu_0 \mu_r (\sigma \frac{\partial \vec{A}}{\partial t} - \vec{j}^s) \quad (11.1)$$

Induction coil carries sinusoidal current, Hence eq(11.1) can be written as,

$$\nabla^2 A = \mu_0 \mu_r (\sigma \omega \vec{A} - \vec{j}^s) \quad (11.2)$$

For 2-D axisymmetric geometry shown in figure 2(a) and using cylindrical coordinates, eq (11.2) can be written as,

$$\text{In induction coil } \frac{\partial^2 A_\theta}{\partial r^2} + \frac{1}{r} \frac{\partial A_\theta}{\partial r} + \frac{\partial^2 A_\theta}{\partial z^2} - \frac{A_\theta}{r^2} = j\omega \mu_0 \mu_r \sigma A_\theta - \mu_0 \mu_r j^s \quad (12.1)$$

$$\text{In Workpiece } \frac{\partial^2 A_\theta}{\partial r^2} + \frac{1}{r} \frac{\partial A_\theta}{\partial r} + \frac{\partial^2 A_\theta}{\partial z^2} - \frac{A_\theta}{r^2} = j\omega \mu_0 \mu_r \sigma A_\theta \quad (12.2)$$

$$\text{In vacuum/air } \frac{\partial^2 A_\theta}{\partial r^2} + \frac{1}{r} \frac{\partial A_\theta}{\partial r} + \frac{\partial^2 A_\theta}{\partial z^2} - \frac{A_\theta}{r^2} = 0 \quad (12.3)$$

In these equations, θ , z , r are the Cylindrical coordinates, A_θ is the θ Component of the magnetic vector potential (V.sec/m), ω is the Angular frequency of coil current (rad/sec).

2.3 Numerical analysis

Finite Element Method (FEM) is used to solve the eq (12.1), (12.2) & (12.3) in geometry given in figure 2(a). In this method, Solution domain is discretized into number of discrete sub domain or elements. After discretization, integral formulation is obtained by using Galerkin technique, which is known as weak form. After that, algebraic equations for each element are obtained in matrix form. Assembling of all element equations gives the global matrices [18] as shown below

$$[K]\{A\} + [H]\{A\} = \{J\} \quad (13)$$

In this equation, $[K]$ is the stiffness matrix, $[H]$ is the Mass matrix,

{A} is the Magnetic vector Potential, {J} is the Electrical current density.

Eq (13) is solved by using suitable boundary conditions and forcing function. Once, magnetic vector potential is determined, then other quantities like, coil resistance, reactance, voltage, and work piece power are computed.

2.4 Simulation

Simulation is done in three steps i.e. preprocessing, processing & post processing [1], [19]. In preprocessing, 2-D axisymmetric geometry shown in figure 2(a) is used for simulation. Materials and their properties given in table-I and table –II are assigned to different domains. Boundary conditions are specified as per table -III. Current is used as forcing function. Triangular elements are used for domain discretization. Mesh is refined on the surface of induction coil and workpiece as shown in the figure 2(b) [19]. Induction coil carries sinusoidal current, therefore frequency domain study is done for this analysis [16]. In processing step, magnetic vector potential is computed in different domains as shown in figure 2(c). In post processing step, other process related quantities like Magnetic flux density, Coil resistance, reactance, voltage and workpiece power are computed.

Table-I. Workpiece dimension and properties

Sr. No.	Work Piece	Description
1.	Material	Graphite
2.	Outer Diameter	160 mm
3.	Inner Diameter	117.5 mm
4.	Height	180 mm
5.	Electrical Conductivity at 273 ⁰ K	1.42653X10 ⁵ S/m
6.	Electric permittivity	1
7.	Magnetic permeability	1

Table-II Induction coil dimensions and properties

Sr.No.	Induction coil	Description
1.	Material	Copper
2.	Inside diameter	215mm
3.	Outside diameter	247mm
4.	Height	200mm
5.	Coil tube diameter	16mm
6.	Coil tube thickness	2mm
7.	No. of turn	9
8.	Electrical conductivity at 273 ⁰ K	5.998X10 ⁷ S/m
9.	Electric permittivity	1
10.	Magnetic permeability	1

Table-III Boundary condition and forcing function

Sr.No.	Boundary condition	Description
1.	Outer boundary	$A=0$
2.	Asymmetry axis	$\frac{\partial A}{\partial n} = 0$

Table-IV Lead cable specification

Sr no	Lead Cable	Description
1	Material	Copper
2	Length	3.61 m
3	Outer diameter	0.025m
4	Thickness	0.001 m
5	Insulation gap	0.015m

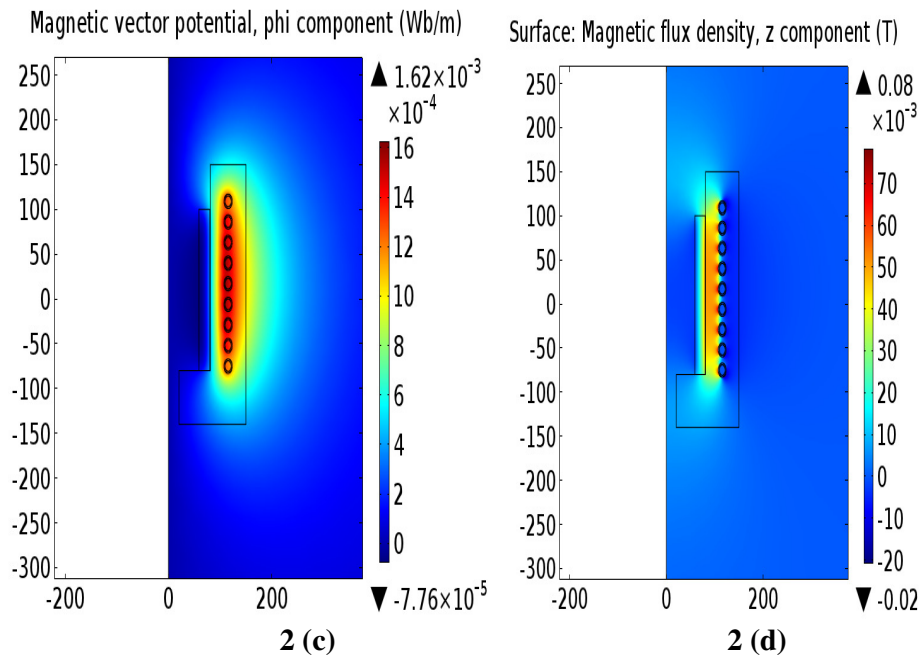
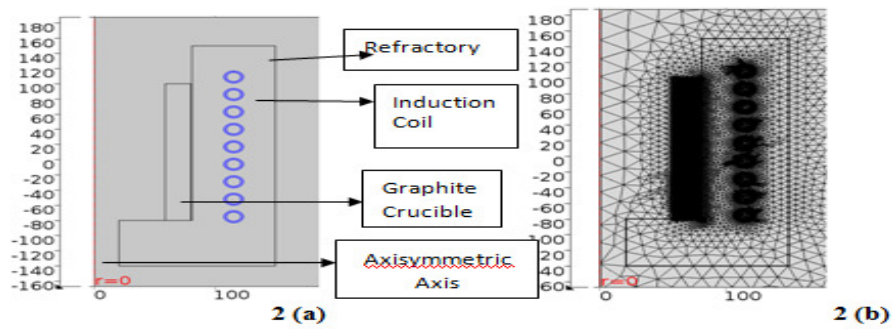


Figure 2(a). Axisymmetric geometry, 2(b) Meshing, 2(c). Magnetic vector potential at 6.55 kHz, 2(d) Magnetic flux density at 6.55 kHz

2.5 Experiment

Experiments were carried out on vacuum induction melting furnace. Schematic diagram of furnace is shown in the figure (3). 40 kW, 5 kHz, 400 V Power source was connected to the induction coil. During experiment, various parameters such as Coil current, coil voltage were measured and recorded at different frequency as shown in figure 4. High frequency current was measured by rogowski coil [20]. During experiment, Vacuum below 100 μ bar and cooling water pressure more than 2 kg/cm² were maintained.

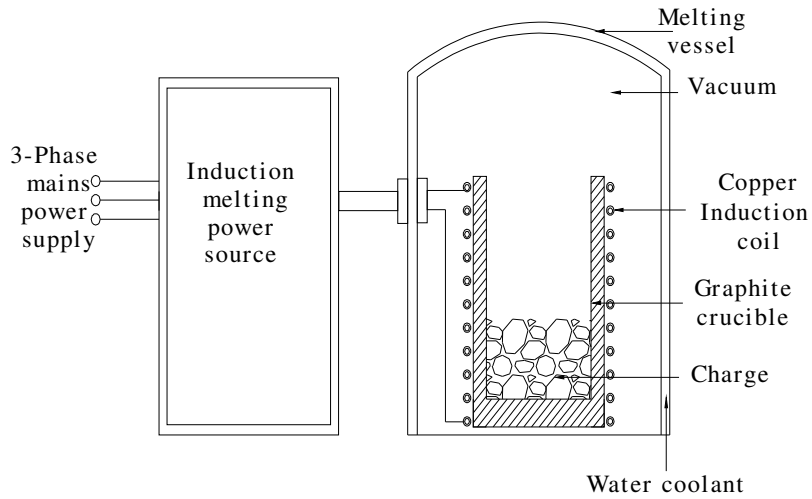


Figure (3). Schematic diagram of Uranium melting

3. RESULT AND ANALYSIS

Experimental results are shown in the figure (4). From figure (4), it is observed that resonance frequency of series RLC circuit is approximately (6 kHz). As power source output frequency moves towards resonance frequency, induction coil voltage and current increase.

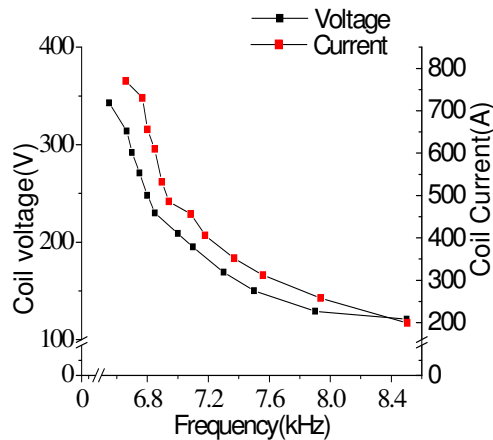


Figure (4). Coil voltage and coil current during experiment

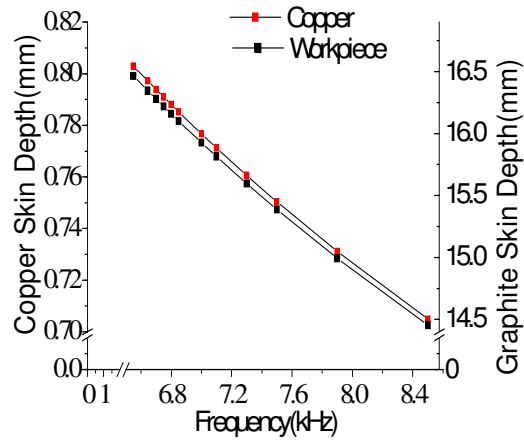
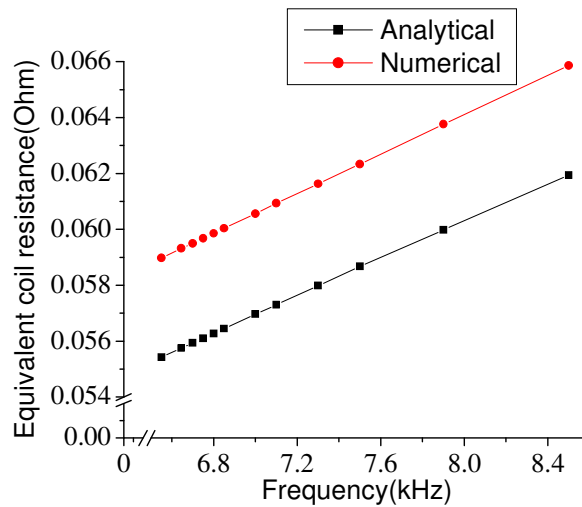
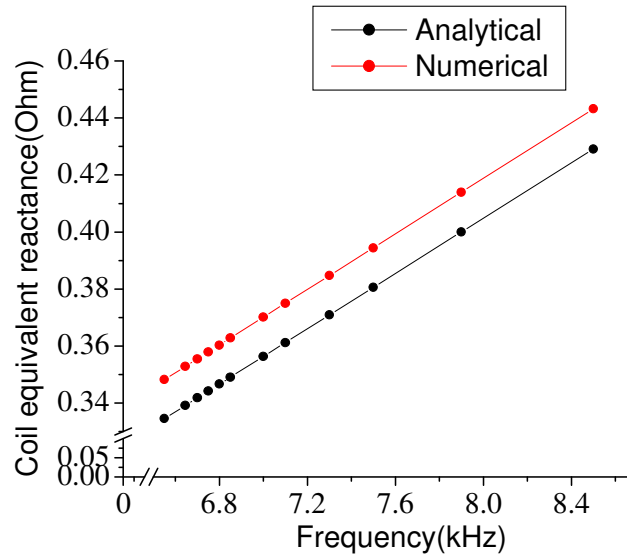


Figure (5). Skin depth at different frequency

In figure (5), it is observed that skin depth in graphite is 20 times more than copper due to high resistivity of graphite. Figure 6(a) and 6 (b), show the comparison of analytically and numerically calculated equivalent coil resistance and reactance. The difference between analytical and numerical resistance and reactance values are less than 7 % and 4 % respectively in specified frequency range.



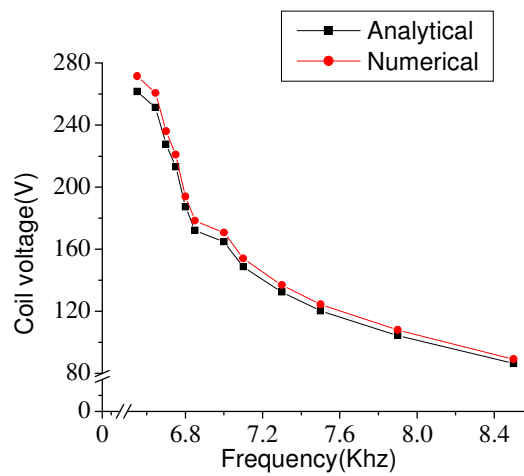
6 (a)



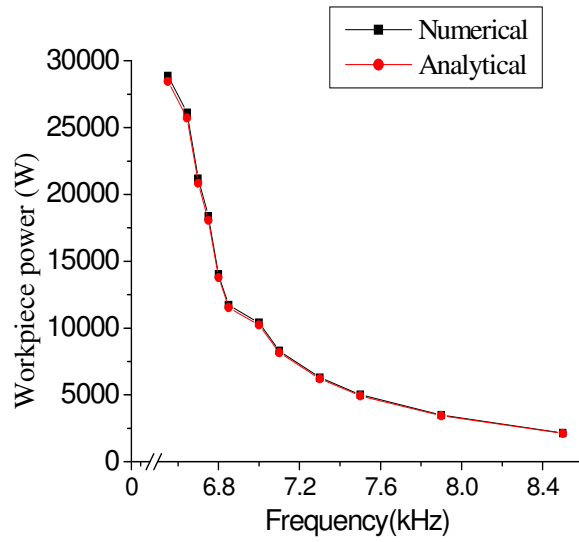
6 (b)

Figure 6(a) coil and workpiece equivalent resistance, 6(b) Coil and workpiece equivalent reactance

From figure 7 (a) and (b), it is observed that analytical and numerical calculated coil voltage and workpiece power are in good agreement and difference is less than 4% for coil voltage and less than 2 % for workpiece power in specified frequency range.



7 (a)



7 (b)

Figure (7) (a) Coil voltage, (7) (b) workpiece power calculated by analytical and numerical methods

Figure (8) shows the workpiece and coil power calculated by eq (7.1) and (7.2) at different frequency. These data are used to calculate the coil efficiency at different frequencies and found that coil efficiency is ~81%.

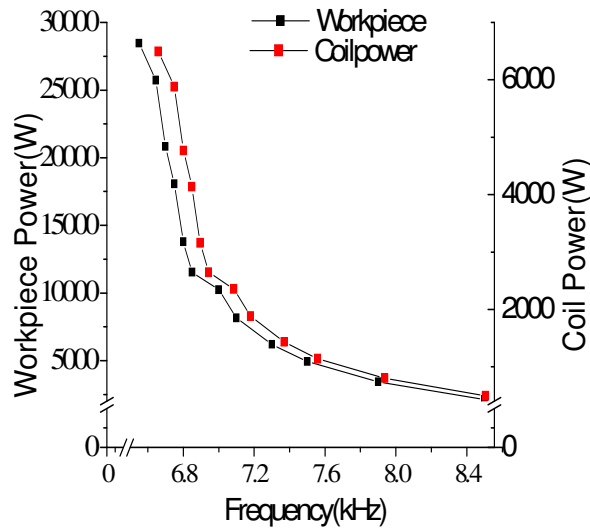


Figure (8) Coil and work piece power at different frequency

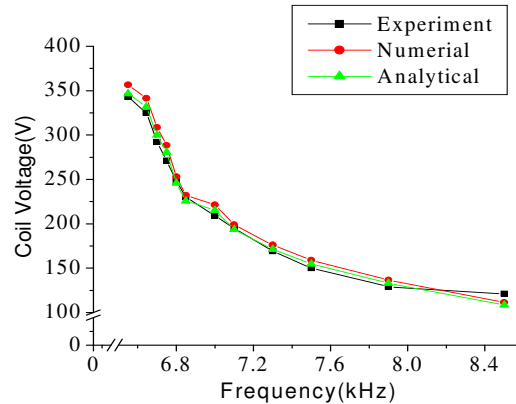


Figure (9) Analytically, numerically and experimentally obtained coil voltage

After validation of analytical and numerical model of induction heating process, experiment was conducted to validate the coil voltage calculated by analytical and numerical method. Figure (9) shows the comparison of analytical, numerical and experimental coil voltage. In this comparison, lead impedance is included during analytical and numerical computation, because during experiment, coil voltages are measured at power source output terminal. From figure (9), it is observed that results are in good agreement.

4. CONCLUSION

Mathematical modeling and simulation of electromagnetic induction phenomenon in induction heating process were carried out and results were validated by analytically obtained results. Experiments were conducted to validate the coil voltage obtained by analytical and numerical methods at different frequencies. Analytical and numerically calculated workpiece power at different frequencies is very much close to each other and that is the main concern of induction heating system designer. This model can be applied to optimize the coil parameters to get the desired results in induction heating of different kind of materials and avoid the tedious experiments. This model helps to understand the dynamics of induction heating process in depth. As these analyses are restricted only to electromagnetic part of induction heating, this can be further coupled to the power source for transient analysis and heat transfer physics to find out temperature profile in workpiece.

5. REFERENCES

- [1] Valery Rudnev, Don loveless, Raymond Cook, Micah Black, "Handbook of Induction heating", INDUCTOHEAT, Inc., Madison Heights, Michigan, U.S.A.
- [2] E.J Davies and P.G. Simpson, Induction Heating Handbook. McGraw Hill, 1979.
- [3] Phuong-Xuan Dang, "Improving the energy efficiency by process parameter optimization approach: a case study of induction heating. International journal of renewable energy and environmental engineering", ISSN2348-0157, Vol.01, No.01, October 2013.

- [4] C Chabodez, S Clain, R.Glardon, D Mari, J.Rappaz, M. Swierkosz, "Numerical modeling in induction heating for axisymmetric geometries", IEEE transactions on Magnetics.Vol33, No.1 January 1997, P 739-745.
- [5] Jiin-yung Jang, Yu-We Chiu, "Numerical and experimental thermal analysis for a metallic hollow cylinder subjected to step wise electromagnetic induction heating", applied thermal engineering 27(2007), 1883-1894.
- [6] K. sageghipour, J.A Dopkin,K.Li," A computer aided finite element/experiment analysis of induction heating process of steel, computer in industries,28(1996) 195-205.
- [7] Q.-S.Chen, P. Gao, W.R.Hu, "Effects of induction heating on temperature distribution and growth rate in large size Sic growth system, journal of crystal growth 266(2004) 320-326.
- [8] Mohammad Hosin, Tavakoli, Hosin Karbasachi, Feridoun Samavat, "Influence of workpiece height on induction heating process", Mathematical and computer modeling, Elsevier journals.2011.
- [9] Mark William Kennedy, Shahid Akhtar, Jon Arne Bakken,, Ragnhild E.Aune, "Review of Classical Design Methods as applied to aluminum billet heating with induction coils", EPD congress, San Diego, California, February 27-March 3(2011),702-722.
- [10] Lisiate Takau, Pat Bodger, "Low frequency modeling of induction heater using series equivalent circuit, transformer equivalent circuit, and finite element analysis", Australasian universities power engineering conference, AUPEC 2013.Hobart,TAS, Australia,29 September-3 October 02013, p-1-6.
- [11] Mark William Kennedy, Shahid Akhtar, Jon Arne Bakken,, Ragnhild E.Aune, " Analytical and FEM modeling of aluminum billet induction heating with experimental verification", TMS(The mineral, Metals & Materials Society),2012
- [12] J Acero, J.M. Burdio, L.A. Barragan, J.I.Artigas, R. Alosa, "An electromagnetic based model for calculating the efficiency in domestic induction heating appliances," Power electronic specialist conference 2006, PESC06, 37th IEEE, P, 1-6.
- [13] Milton Abramowitz, Irene A Stegun, "Handbook of mathematical functions, national bureau of standard," Applied Mathematics Series.55, December 1972.
- [14] C.L. Wadhwa, " Electrical power systems," New age international publishers, New Delhi,2014
- [15] Andrzej Krawczyk, John A. Tegopoulos, "Numerical modeling of eddy current," Oxford science publications, P-17.
- [16] K.Djellabi, Meh Latreche, "Induction heating process design using Comsol multiphysics software version 4.2a," International journal of electrical, computer, electronics and communication engineering, vol8 no 1 2014
- [17] Sun Yefei, Sun Jing, Niu Dongjie, "Numerical simulation of induction heating of steel bar with nonlinear material properties," Proceeding of IEEE conference on automation and logistic Shenyang, China August 2009.
- [18] Huang, Hou-cheng, "Finite element analysis of heat transfer: theory and software," Springer verlo, London, 1994.
- [19] Ion Carstea, Daniela Carstea, Alexandru Adrian Carstea, "A domain decomposition approach for coupled field in induction heating device," 6th WEEAS international conference on system science and simulation in engineering, Venice, Italy, November 21-23,2007,P63-70
- [20] D.A.Ward And J.La.T.Exon, "Using Rogowski coils for transient current measurements", Engineering Science and Education Journal, June 1993.